Mathematical modelling and numerical simulation of a glow-plug*

L. Formaggia[♯], S. Micheletti[♯], R. Sacco[†], A. Veneziani[♯]

12th January 2006

[♯] MOX– Modellistica e Calcolo Scientifico
Dipartimento di Matematica "F. Brioschi"
Politecnico di Milano
via Bonardi 9, 20133 Milano, Italy
{luca.formaggia,stefano.micheletti,alessandro.veneziani}@polimi.it

[†] Dipartimento di Matematica "F. Brioschi"
Politecnico di Milano
via Bonardi 9, 20133 Milano, Italy
riccardo.sacco@polimi.it

Keywords: Non-linear heat transfer; Mixed finite elements; Quasi-Newton methods.

AMS Subject Classification: 65M60, 35K60, 35K57, 80A20, 90C53

Abstract

In this work we derive a mathematical model that describes the working of a glow-plug of the type used in Diesel engines to preheat the air-diesel fuel mixture. The proposed model consists of a time dependent one dimensional partial differential equation which incorporates the electro-thermal interaction between the electric current flowing in the plug and the temperature. It has been obtained by integrating the heat equation on each section of the plug, assuming axial symmetry and using thermal equilibrium relation in the radial direction. The problem is highly non-linear because of the radiation boundary conditions and the dependence on temperature of several parameters. In particular, heat is generated by an electric resistance whose characteristic strongly depends on temperature. We have adopted a quasi-Newton treatment of the non-linear term and a mixed finite element formulation for the linearized problem. Time advancing has been carried out using a semi-implicit Euler scheme. Several numerical simulations have been carried in order to assess the validity of the model, whose predictions have been compared with available experimental data.

*This work has been carried out under the Contract *Modellazione Matematico-Numerica Bidimensionale per la Progettazione e l'Ottimizzazione di una Candeletta di Preriscaldo. Simulazione in Condizioni Normali e di Cortocircuito*, between Politecnico di Milano - Dipartimento di Matematica "F. Brioschi, and Federal Mogul Ignition S.r.l.. The research has been partly supported by Project PRIN-2004 *Numerical adaptivity and adaptivity of models for partial differential equations.*

1 Introduction

A glow-plug is a device that heats up the air-fuel mixture in a Diesel engine combustion chamber with a twofold objective. The first is to facilitate the start up even at low external temperatures. The second is to reduce pollution emissions by favoring combustion.

A typical glow-plug geometry is shown in Fig. 1. It consists of an external

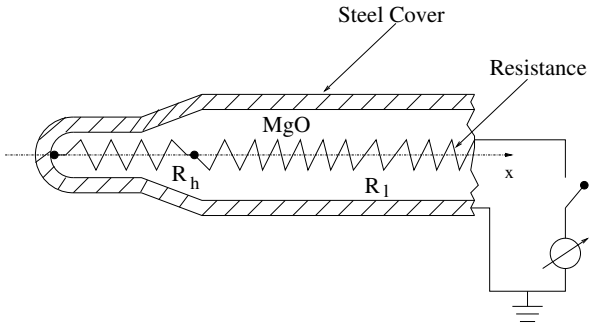

Figure 1: Geometry of a glow-plug (not in scale)

cover, typically made of steel, which contains an insulating material, normally MgO compacted powder. Immersed in the powder we have the resistive element, typically made by two electric resistances connected in series and denoted as the *heating* and the *controlling* (or limiting) resistance, respectively. They are indicated by R_h and R_l in Fig. 1 and are usually made of a thin coiled filament of electrical conducting material. At start-up, an electric voltage is supplied at one end of the controlling resistance, which is connected to a metallic stand (not shown in the figure), so that an electric current starts flowing through the coil which is soldered at the other end to the tip of the glow-plug (which acts as electrical ground). The resistances are chosen so that at ambient temperature $R_h \gg R_l$. Thus, most of the heat is generated by Joule effect in the heating resistance, producing a fast temperature rise at the tip of the glow-plug. However, the material in the controlling element is chosen so that R_l is strongly dependent on the temperature and, in particular, satisfies $\frac{dR_l}{dT} > 0$. Therefore, as the temperature in the rear of the glow-plug rises because of thermal conduction, the controlling resistance increases, eventually equaling (if not overtaking) R_h. This results in a more evenly distributed heat generation at steady-state, with a temperature profile more homogeneous along the glow-plug. This situation is appropriate after start up, when the plug operates as preheating element for the air-diesel fuel mixture to reduce pollution emissions. Clearly, heat is dissipated mainly via radiation at the cover surface.

The objective of this work was to derive a simplified, yet effective, one dimensional model for the glow plug, by exploiting its (almost) axisymmetric geometry (the spiralling form of the electric resistance deviates the domain from a perfect

axial symmetry). The motivation was to have a computationally efficient tool able to aid the design of novel glow-plug models. This goal was rather challenging because of the presence of non-linear terms and the need to accurately capture the transient. Furthermore, we had to account for the variation of temperature in the radial direction r even if no differential equation along r was to be solved.

Some experimental research has been carried out in the recent past to investigate the effectiveness of glow plug heating in ethanol based engines [4, 9], or the use of glow-plugs for new concept natural gas engines [8]. However, the numerical modelling and simulation of the heating process in a glow plug is a rather novel application and, to our knowledge, this is the first attempt to this direction.

Our starting point was the system of equations governing the temperature T and the electric potential V. To describe them we first denote by $\Omega_O \subset \mathbb{R}^3$, $\Omega_G \subset \mathbb{R}^3$ and $\Omega_S \subset \mathbb{R}^3$ the parts of the computational domain Ω occupied by the MgO compacted powder, the covering steel and the heating resistive element (in the form of a coil), respectively. We have assumed that the coil diameter is small compared with the glow-plug diameter, so that Ω_S is in fact a one-dimensional curve immersed into Ω_O, as shown in Figure 1. We then have

$$\begin{cases} C\dfrac{\partial T}{\partial t} - \operatorname{div}(\kappa \nabla T) = q(V) & \text{in } \Omega\,, \\ -\dfrac{\partial}{\partial l}(\rho^{-1}\dfrac{\partial V}{\partial l}) = 0 & \text{in } \Omega_S\,, \end{cases} \tag{1}$$

where t indicates the time and l the arc length coordinate along the coil, C is the thermal capacity, κ the thermal conductivity, ρ the electric resistivity of the coil, and $q = q(V)$ the power density generated via the Joule effect. The first equation in (1) is the classical heat equation with source term while the second equation enforces the conservation of the electric current inside the conducting coil. Some assumptions have been made, notably:

- all the magnetic phenomena are neglected;
- the coil is assumed to obey Ohm's law and have a negligible inductance, so to neglect the transient term in the second equation.
- the MgO compacted powder is a perfect insulator. Consequently, the steel covering is insulated from the coil.

The quantities C and κ differ in each medium and, in general, depend on temperature. Eqns. (1) are supplemented by appropriate boundary and initial conditions which will be detailed in the sequel of the work. We note that because of the assumptions on Ω_S, $q(V)$ is not an ordinary function and the first equation in (1) has to be interpreted in a distributional sense.

A difficulty of the problem lays in the non linear behavior of the coefficients and of the boundary conditions for the thermal problem, which are dominated by the radiation effect. It is not the aim of the present work to analyze in

depth the mathematical properties of the proposed reduced one dimensional model, this aspect is left to a forthcoming article. Instead, we will describe in detail the steps taken in its derivation and numerical discretisation, as well as the validation of the numerical results against available experimental data. To complete the bibliographical references we mention two recent works on the analysis and numerical simulation of non-linear heat radiation problems, even if set for different applications that the one to hand, namely [6] and [3].

The paper is organized as follows. By the aid of some reasonable hypothesis we have been able to formulate an a-priori radial profile of the temperature, as described in Sect 2. This information is necessary for the derivation of the one-dimensional model carried out in Sect. 3. The specification of the the source term q requires to account for typical coil geometries, this is detailed in Sect. 4. The resulting one dimensional model is governed by a strongly non-linear differential equation. We propose in Sect. 5 a fixed-point scheme of quasi-Newton type for its solution. Mixed finite elements have interesting local conservation properties which are deemed important in this context. This is why they have been selected for the discretisation of the linear kernel, as shown in Sect. 6. Finally, in Sect. 7 we have assessed our numerical procedure both on simple test cases and by comparisons with some experimental data kindly provided by Federal Mogul Ignition S.r.l.

2 The radial temperature profile

We want to derive a one-dimensional model where the plug temperature T is a function only of the time and of the axial coordinate x. Since we expect a relevant radial variation of the temperature, we have to assume a reasonable a-priori profile for T. To that aim, we will make the following assumptions:

1. the temperature in each cross-section (i.e. at constant x) depends only on the radial coordinate r and satisfies at any time the thermal equilibrium condition in the radial direction. In other words, we neglect thermal inertial effects along the radial direction;

2. the coil may be approximated on each cross-section by a circular linear heat source of radius R_S, coinciding with the average radius of the coil in that section;

3. the thermal conductivities are piecewise constant w.r.t. the radial coordinate, i.e. the characteristics of the materials constituting each sub-domain are homogeneous on each section.

In Fig. 2 we sketch the geometry of a generic cross-section, which is characterized by three geometrical parameters: the average radius of the coil R_S; the radius R_G of the internal surface of the steel covering and the external radius R_E, respectively. Of course, these parameters may still depend on the axial coordinate x. On each cross-section

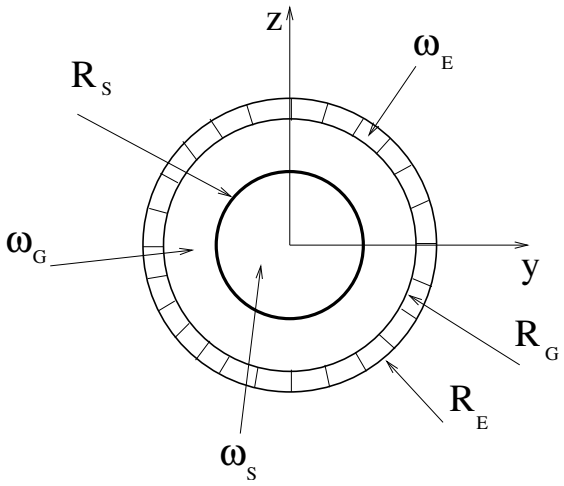

Figure 2: Geometry of the cross-section of the glow plug

$$\omega(x) = \{(r,\theta) : 0 < r < R_E(x), 0 \le \theta < 2\pi\}$$

we can identify the following subsets, see Fig. 2,

$$\begin{aligned}
\omega_S(x) &:= \{(r,\theta) : 0 < r < R_S(x), 0 \le \theta < 2\pi\}, \\
\omega_G(x) &:= \{(r,\theta) : R_S(x) < r < R_G(x), 0 \le \theta < 2\pi\}, \\
\omega_E(x) &:= \{(r,\theta) : R_G(x) < r < R_E(x), 0 \le \theta < 2\pi\}.
\end{aligned}$$

The hypothesis of thermal equilibrium in the radial direction implies that for any fixed $x \in (0, L)$ the temperature T satisfies the steady-state equation

$$-\kappa \frac{1}{r}\left(\frac{\partial}{\partial r} T\right) = 0 \tag{2}$$

in each subset of ω, where

$$\kappa = \begin{cases} \kappa_O & \text{in } \omega_S \cup \omega_G, \\ \kappa_G & \text{in } \omega_E, \end{cases}$$

with κ_O and κ_G indicating the values of the thermal conductivities in the MgO compacted powder and in the steel, respectively. Please note that they may be functions of the temperature. The heat $\hat{q} = \hat{q}(V)$ generated by the coil will be implicitly accounted for in the interface conditions between ω_S and ω_G.

Furthermore, we need to consider the radiation condition

$$-\kappa_G \frac{\partial T}{\partial r}\bigg|_{R_E^-} = e\,\sigma(T_E^4 - T_a^4),$$

on the exterior boundary of ω_E, where T_a is the ambient temperature, here assumed constant. This boundary term implies that the dominant heat transfer

mechanism on the external surface of the glow plug is due to radiation, a reasonable hypothesis due to the temperatures we are going to consider. However, it is rather simple to add other contributions, for instance linked to convective heat transfer.

By σ we have indicated the Stefan constant and e is the emissivity of steel, under the hypothesis that it behaves like a gray body radiating to infinity (no geometrical factors are taken into account).

To get a manageable problem we use an argument akin to that used in a domain decomposition context [7].

More precisely, to the equations

$$\begin{aligned} -\kappa_O \frac{1}{r}\frac{\partial}{\partial r}\left(r\frac{\partial T}{\partial r}\right) &= 0\,, \quad 0 < r < R_G\,, \\ -\kappa_G \frac{1}{r}\frac{\partial}{\partial r}\left(r\frac{\partial T}{\partial r}\right) &= 0\,, \quad R_G < r < R_E\,, \end{aligned} \tag{3}$$

with boundary conditions

$$-\kappa_O \left.\frac{\partial T}{\partial r}\right|_{0^+} = 0, \quad -\kappa_G \left.\frac{\partial T}{\partial r}\right|_{R_E^-} = e\,\sigma(T_E^4 - T_a^4) \tag{4}$$

we add the following interface conditions,

$$\begin{aligned} &T|_{R_G^-} = T|_{R_G^+} = T_G, \qquad\qquad T|_{R_S^-} = T|_{R_S^+} = T_S \\ &-\kappa_O \left.\frac{\partial T}{\partial r}\right|_{R_G^-} = -\kappa_G \left.\frac{\partial T}{\partial r}\right|_{R_G^+}. \end{aligned} \tag{5}$$

Here T_S, T_G and T_E indicate the temperatures at $r = R_S$, $r = R_G$ and $r = R_E$, respectively, while $T|_{R^\pm} = \lim_{r \to R^\pm} T(r)$.

The first boundary condition is derived by symmetry considerations. Notice that at $r = R_S$ we expect a finite jump of the heat flux due to the heat power generated by the coil. The value of this jump cannot be imposed at this stage, since part of the heat generated by the coil is transferred along the x direction, and the precise amount cannot be computed until an equation for the heat transport in the x direction has been derived. Nevertheless, we will now show how, by using the previous relations, the temperature profile in each cross-section can be written as a function of a single parameter, which we have here taken to be the external temperature T_E. The latter will then be the main dependent variable of our one dimensional problem.

The general solution of each equation of system (3) is in the form $T(r) = a + b\log r$, and the constants a, b may be determined thanks to the interface and boundary conditions. In particular, by imposing the continuity conditions at the interfaces $r = R_S$, $r = R_G$ and $r = R_E$ one obtains that T_G may expressed as the following convex average of T_S and T_E,

$$T_G = \frac{\frac{\kappa_O}{\log\frac{R_G}{R_S}} T_S + \frac{\kappa_G}{\log\frac{R_E}{R_G}} T_E}{\frac{\kappa_O}{\log\frac{R_G}{R_S}} + \frac{\kappa_G}{\log\frac{R_E}{R_G}}}\,. \tag{6}$$

The radiation condition enables us to express T_G as a function of only T_E. Indeed,

$$-\kappa_G \frac{\partial T}{\partial r}\bigg|_{R_E^-} = e\,\sigma(T_E^4 - T_a^4) \Longrightarrow -\frac{\kappa_G}{R_E}\frac{T_E - T_G}{\log\frac{R_E}{R_G}} = e\sigma(T_E^4 - T_a^4)\,.$$

Thus, we have

$$T_G = T_E + \frac{e\,\sigma R_E}{\kappa_G}\log\frac{R_E}{R_G}(T_E^4 - T_a^4)\,. \tag{7}$$

Finally, the combination of (6) and (7) yields

$$T_S = T_E + e\,\sigma R_E\left(\frac{\log\frac{R_E}{R_G}}{\kappa_G} + \frac{\log\frac{R_G}{R_S}}{\kappa_O}\right)(T_E^4 - T_a^4)\,, \tag{8}$$

which provides us with the temperature of the coil T_S as a function of T_E.

The temperature profile in the region $0 < r < R_S$ turns out to be constant and equal to T_S, due to the first relation in (4) and the continuity of heat flux at $r = R_G$.

Thus, the complete temperature profile is given on each section $\omega(x)$ by

$$T(r) = \begin{cases} T_S, & 0 \le r < R_S\,, \\ T_S + (T_G - T_S)\dfrac{\log\frac{r}{R_S}}{\log\frac{R_G}{R_S}}, & R_S \le r < R_G\,, \\ T_G + (T_E - T_G)\dfrac{\log\frac{r}{R_G}}{\log\frac{R_E}{R_G}}, & R_G \le r \le R_E\,, \end{cases} \tag{9}$$

with T_G and T_S given by (7) and (8), respectively.

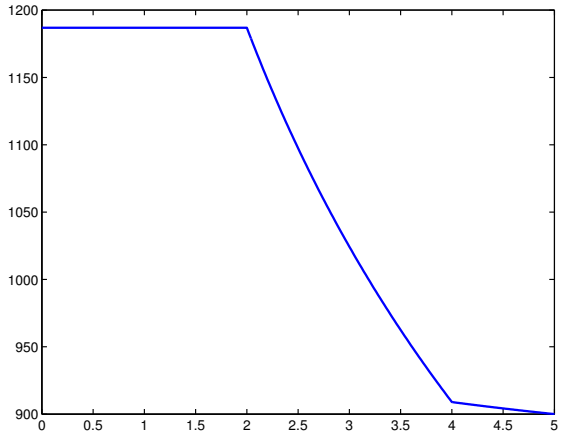

Figure 3: Temperature profile w.r.t. radial coordinate in a generic cross-section

Figure 3 shows the temperature profile corresponding to the following (realistic) values $T_E = 900\,^\circ\mathrm{C}$, $T_a = 20\,^\circ\mathrm{C}$, $e = 0.75$, $\kappa_O = 1$ W/(mK), $\kappa_G = 10$

W/(mK), $R_S = 2$ mm, $R_G = 4$ mm, $R_E = 5$ mm, and $\sigma = 5.67 \cdot 10^{-8}$ W/(m^{2}K^4). Notice that the temperature at the coil is about $T_S = 1187\,^\circ$C, and that the largest temperature drop is located across the MgO compacted powder, as expected. We may also note the discontinuities in the derivatives, due to the change of material conductivity at $r = R_G$ and to the coil heat flux at $r = R_S$.

3 An equation for the axial temperature profile

We are now in the position to derive an equation for the axial distribution of the temperature with T_E as our main variable. Again, we will assume that $x \in [0, L]$, L being the length of the glow plug, with $x = 0$ corresponding to the tip of the plug. In fact, the point $x = 0$ corresponds to the soldering between the coil and the cover (see Figure 4).

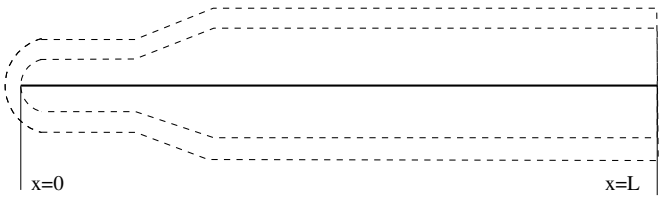

Figure 4: The coordinate system chosen for the derivation of the one dimensional model

Let us recall that the divergence operator in cylindrical coordinates for an axisymmetric quantity T is given by

$$\mathrm{div}(\kappa \nabla T) = \frac{1}{r}\frac{\partial}{\partial r}\left(r\kappa\frac{\partial T}{\partial r}\right) + \frac{\partial}{\partial x}\left(\kappa\frac{\partial T}{\partial x}\right), \tag{10}$$

and integrate the first differential equation in (1) on the generic cross-section $\omega(x)$ with $x \in (0, L)$. To account for the different material characteristics we split the integration with respect to the radial coordinate r in the two intervals $[0, R_G]$ and $[R_G, R_E]$. By exploiting the hypothesis of axial symmetry and (for the sake of conciseness) by dividing both members by 2π, we obtain

$$\begin{aligned} & \frac{\partial}{\partial t}\left(C_O \int_0^{R_G(x)} Tr\,dr + C_G \int_{R_G(x)}^{R_E(x)} Tr\,dr\right) \\ - & \int_0^{R_G(x)} \frac{\partial}{\partial x}\left(\kappa_O \frac{\partial T}{\partial x}\right) r\,dr - \int_{R_G(x)}^{R_E(x)} \frac{\partial}{\partial x}\left(\kappa_G \frac{\partial T}{\partial x}\right) r\,dr \\ - & r\kappa_O \frac{\partial T}{\partial r}\bigg|_0^{R_G(x)} - r\kappa_G \frac{\partial T}{\partial r}\bigg|_{R_G(x)}^{R_E(x)} = Q\,, \end{aligned}$$

C_O, C_G being the (constant) values of the thermal capacities in the MgO powder and in the steel, respectively, while Q is the heat power per unit length generated by the coil (divided by 2π), which we will model in Section 4. We have indicated explicitly the possible dependence of the geometry with x.

We now exploit the boundary and interface conditions (4) and (5) to write

$$\begin{aligned} & \frac{\partial}{\partial t}\left(C_O\int_0^{R_G(x)} Tr\,dr + C_G\int_{R_G(x)}^{R_E(x)} Tr\,dr\right) \\ - & \int_0^{R_G(x)}\frac{\partial}{\partial x}\left(\kappa_O\frac{\partial T}{\partial x}\right)r\,dr - \int_{R_G(x)}^{R_E(x)}\frac{\partial}{\partial x}\left(\kappa_G\frac{\partial T}{\partial x}\right)r\,dr \\ + & R_E e\,\sigma(T_E^4 - T_a^4) = Q\,. \end{aligned} \tag{11}$$

To handle the problem in a more convenient way, we introduce the quantities $\overline{T}_O^A$ and $\overline{T}_G^A$, defined as

$$\overline{T}_O^A = \int_0^{R_G} Tr\,dr, \qquad \overline{T}_G^A = \int_{R_G}^{R_E} Tr\,dr. \tag{12}$$

A direct computation using (9) yields

$$\begin{aligned} \overline{T}_O^A(x;T_E) &= \beta_O(x)T_E + \alpha(x)\gamma_O(x;T_E)T_E^4 - \alpha(x)\gamma_O(x;T_E)T_a^4\,, \\ \overline{T}_G^A(x;T_E) &= \beta_G(x)T_E + \alpha(x)\gamma_G(x;T_E)T_E^4 - \alpha(x)\gamma_G(x;T_E)T_a^4\,, \end{aligned} \tag{13}$$

where the coefficients α, β_O, β_G, γ_O and γ_G are defined by

$$\begin{aligned} &\alpha(x) = R_E(x)e\,\sigma\,,\ \beta_O(x) = \frac{1}{2}R_G(x)^2\,,\ \beta_G(x) = \frac{1}{2}(R_E(x)^2 - R_G(x)^2)\,, \\ &\gamma_O(x;T_E) = \frac{1}{2\kappa_G(T_E)}\left[R_G(x)^2\log\frac{R_E(x)}{R_G(x)} + \frac{\kappa_G(T_E)}{2\kappa_O(T_E)}(R_G(x)^2 - R_S(x)^2)\right]\,, \\ &\gamma_G(x;T_E) = \frac{1}{2\kappa_G(T_E)}\left[\frac{1}{2}(R_E(x)^2 - R_G(x)^2) - R_G(x)^2\log\frac{R_E(x)}{R_G(x)}\right]\,. \end{aligned} \tag{14}$$

In the previous relations with the notation $(x;T_E)$ we wanted to put into evidence the parametric dependence on x, through the (known) geometrical dimensions R_S, R_G and R_E (we have assumed that the thermal properties of the MgO powder and the steel cover are constant w.r.t x). Clearly, being T_E itself a function of x and t we will have in general

$$\frac{\partial f}{\partial x}(x;T_E(x,t)) = \frac{\partial f}{\partial x}\Big|_{T_E}(x;T_E(x,t)) + \frac{\partial f}{\partial T_E}\Big|_x(x;T_E(x,t))\frac{\partial T_E}{\partial x}(x,t).$$

where $\frac{\partial f}{\partial x}\big|_{T_E} = 0$ whenever R_E, R_G and R_S are constant. This notation will be useful since in the following derivation we want to discern the terms linked to the geometry.

Since $\forall x \in [0,L]$ it holds that $\Phi \geq R_E > R_G \geq R_S \geq 0$, being Phi the maximum plug radius, and moreover $K_G > 0$, we may state the following properties

$$\begin{aligned} &\lim_{R_E\to 0^+}\alpha = \lim_{R_E\to 0^+}\beta_0 = \lim_{R_E\to 0^+}\beta_G = \lim_{R_E\to 0^+}, \gamma_O = \lim_{R_E\to 0^+}\gamma_G = 0 \\ &\lim_{R_G\to 0^+}\alpha = R_E e\,\sigma, \quad \lim_{R_G\to 0^+}\beta_0 = 0, \quad \lim_{R_G\to 0^+}\beta_G = \frac{R_E^2}{2}, \\ &\lim_{R_G\to 0^+}\gamma_O = 0, \quad \lim_{R_G\to 0^+}\gamma_G = \frac{R_E^2}{4\kappa_G}. \end{aligned}$$

Furthermore, we may reasonably assume that R_E, R_G and R_S are (at least) C^0 functions of x and that κ_E and κ_G are bounded C^∞ functions of T. Consequently, $\overline{T}_O^A$ and $\overline{T}_G^A$ depend continuously on geometry variations and are C^∞ bounded functions with respect to T_E.

Let us note that $\overline{T}_O^A$ and $\overline{T}_G^A$ are linked to the mean temperatures $\overline{T}_O$ and $\overline{T}_G$ in $\omega_S \cup \omega_G$ and ω_E, respectively, by the relation

$$\overline{T}_O^A = \frac{R_G^2}{2}\overline{T}_O, \qquad \overline{T}_G^A = \frac{R_E^2 - R_G^2}{2}\overline{T}_G,$$

yet it is more convenient for the derivation of our model to use the former variables.

We recall the following relation, valid for any sufficiently smooth functions $T = T(r,x)$ and $k = k(x)$,

$$\begin{aligned}\int_{R_1(x)}^{R_2(x)} \frac{\partial}{\partial x}\left[\kappa(x)\frac{\partial}{\partial x}[rT(r,x)]\right]\,dr &= \frac{d}{dx}\left[\kappa(x)\frac{d}{dx}\int_{R_1(x)}^{R_2(x)} rT(r,x)\,dr\right]\\ &+\frac{\kappa(x)}{2}\dot{R}_1^2(x)\frac{dT}{dx}(R_1(x),x) - \frac{\kappa(x)}{2}\dot{R}_2^2(x)\frac{dT}{dx}(R_2(x),x)\\ &+\frac{1}{2}\frac{d}{dx}\left[\kappa(x)\big(T(R_1(x),x)\dot{R}_1^2(x) - T(R_2(x),x)\dot{R}_2^2(x)\big)\right], \end{aligned} \tag{15}$$

where $\dot{R} = \frac{dR}{dx}$ and $\dot{R}^2 = \frac{dR^2}{dx} = 2R\frac{dR}{dx}$. We exploit this relation in (11) and recall the definitions in (12) to derive the following differential equation

$$\frac{\partial}{\partial t}C(x;T_E) - \frac{\partial}{\partial x}[K(x;T_E)] + \alpha T_E^4 - G_0(x;T_E) - \frac{\partial}{\partial x}G_1(x;T_E) = Q + \alpha T_a^4\,, \tag{16}$$

where the dependence on the time variable is understood and the parametric dependence on x is only due to geometry deviations from a circular cylinder. We have introduced the quantities

$$C(x;T_E) = C_O\overline{T}_O^A(x;T_E) + C_G\overline{T}_G^A(x;T_E), \tag{17}$$

and

$$K(x;T_E) = \kappa_O(T_E)\frac{\partial\overline{T}_O^A}{\partial x}(x;T_E) + \kappa_G(T_E)\frac{\partial\overline{T}_G^A}{\partial x}(x;T_E), \tag{18}$$

which represent the stored heat and heat flux per unit length, respectively, while

$$G_0(x;T_E) = -(\kappa_O(x) - \kappa_G(x))\frac{\dot{R}_G^2}{2}(x)\frac{\partial T_G}{\partial x}(x;T_E) - \kappa_G(x)\frac{\dot{R}_E^2}{2}(x)\frac{\partial T_E}{\partial x} \tag{19}$$

and

$$G_1(x;T_E) = -(\kappa_O(x) - \kappa_G(x))\frac{\dot{R}_G^2}{2}(x)T_G(x;T_E) - \kappa_G(x)\frac{\dot{R}_E^2}{2}(x)T_E(x;T_E). \tag{20}$$

In the case of a cylindrical glow plug (16) simplifies into

$$\frac{\partial}{\partial t}C(x;T_E) - \frac{\partial}{\partial x}K(x;T_E) + \alpha T_E^4 = Q + \alpha T_a^4\,, \tag{21}$$

for $x \in (0, L)$ and $t > 0$.

In the following we will indicate the additional terms in (16) by f_g, i.e.

$$f_g = G_0 + \frac{\partial}{\partial x} G_1.$$

We point out that the expression for K contains first derivatives of T_E., thus (16) and (21) are in fact second-order differential equations w.r.t x. Note also that the term G_0 acts like a 'transport operator' whose advection field is linked to geometry variations. Indeed, it vanishes for cylindrical geometries.

We need to complement the differential equation with proper boundary conditions. Typically, the temperature at $x = L$ may be taken constant, since the heat transfer towards the engine head, kept at constant temperature, is very high. At the tip $x = 0$ the heat is transferred by radiation through the tip head. Here we make the simplifying assumption of considering the head at a constant temperature, equal to T_E at $x = 0$. If we indicate with S_t the measure of the tip radiating surface, by e its emissivity, and by T_L the temperature imposed at the stub, we have

$$T_E(L, t) = T_L(t), \quad \text{and} \quad S_t e(T_E^4(0, t) - T_a^4) = K(0, T_E). \tag{22}$$

4 Determination of the power generated via joule effect

We need now to make precise the expression for Q in equation (11). Formally we have that $Q = \int_0^{R_G} qr\, dr$, where q is the source term in the first equation of system (1) and has the dimension of power per unit volume ($\mathrm{W/m^3}$). Consequently, Q has the dimension W/m, i.e. of power per unit length. Yet, since the coil has been modeled as a one dimensional manifold, the integral is only formal and Q will be computed here by writing explicitly the equation of thermal balance. In doing that, we will assume that the electric potential V in the second equation of system (1) depends only on x. We will also assume that the coil may be parametrized with respect to x, that is it does not fold over itself. We will indicate with $l = l(x)$ the arc length coordinate, while $S = S(x)$ is the measure of the coil section and $I = I(t)$ the total current flowing along the coil at a given time. The latter does not depend on x since we are neglecting the displacement current and we consider the coil as immersed in a perfectly insulating medium. By Joule's law the heat generated in a portion of coil of length Δl is given by $\frac{\rho}{S} I^2 \Delta l$. Let then apply the following argument. If we integrate the source term q in the (small) interval $\mathcal{V}$, centered in $x* \in (0, L)$ and of length Δx, with $x^* - \frac{\Delta x}{2} \geq 0$ and $x^* + \frac{\Delta x}{2} \leq L$,

$$\mathcal{V} = \{(x, r, \theta),\ x^* - \frac{\Delta x}{2} \leq x \leq x^* + \frac{\Delta x}{2},\ 0 \leq r \leq R_E(x),\ 0 \leq \theta < 2\pi\},$$

and apply the mean value theorem neglecting high order terms with respect to Δx, we obtain that

$$\int_{\mathcal{V}} q\, dV = \frac{\rho(x^*)}{S(x^*)}\, \Delta l\, I^2 = \frac{\rho(x^*)}{S(x^*)}\, \frac{dl}{dx}(x^*)\, I^2\, \Delta x = R_{\Delta l}(x^*) I^2,$$

where $R_{\Delta l} = \dfrac{\rho(x)}{S(x)}\, \Delta l$ is the total resistance of the coil. Now, by definition $Q(x^*) = \lim_{\Delta x \to 0} \frac{1}{2\pi \Delta x} \int_{\mathcal{V}} q\, dV$, therefore, dropping the affix $*$, we finally obtain that

$$Q(x) = \frac{\rho(x)}{2\pi S(x)}\, \frac{dl(x)}{dx}\, I^2, \quad x \in (0, L).$$

Here, dl/dx is the coil length per unit axial length whose derivation for the most common coil geometries will be illustrated in the Appendix. Since I is not directly available, we need to express it as a function of the total drop of the electric potential across the glow-plug and the electric properties of the coil. By applying Ohm's law on the same volume as above, again neglecting high order terms in Δx, we have

$$V(x^* + \frac{\Delta x}{2}) = V(x^* - \frac{\Delta x}{2}) + I\, R_{\Delta l} = V(x^* - \frac{\Delta x}{2}) + I\, \frac{\rho(x^*)}{S(x^*)}\, \frac{dl}{dx}(x^*)\, \Delta x,$$

which yields, after dividing by Δx and letting $\Delta x \to 0$, to

$$\frac{dV(x)}{dx} = I\, \frac{\rho(x)}{S(x)}\, \frac{dl}{dx}(x)\,.$$

By integrating the above relation along the whole length of the glow-plug we obtain

$$V(L) - V(0) = I \int_0^L \frac{\rho}{S}\, \frac{dl}{dx}\, dx = I \mathcal{R}_C\,,$$

where $\mathcal{R}_C = \int_0^L \frac{\rho}{S}\, \frac{dl}{dx}\, dx$ is the total resistance of the coil. Finally,

$$Q(x) = \left(\frac{\Delta V}{\mathcal{R}_C}\right)^2 \frac{\rho(x)}{2\pi S(x)}\, \frac{dl}{dx}(x)\,. \tag{23}$$

The voltage drop $\Delta V = V(L) - V(0)$ is usually given as the electric potential applied to the glow plug electrodes, and is in general a function of time. We recall that the dependence of ρ with x is related to the different electrical characteristics of the elements that make up the coil and on the fact that the resistivity depends on the temperature. This implies that the law governing the heat generation by the coil is strongly coupled with the equation for heat transfer (16). Indeed the correct behavior of a glow-plug is driven mainly by the different functional dependence of ρ with respect to the temperature in the different parts.

5 Approximation of the axial equation

To make equation (16) amenable to numerical solution we need first to design a procedure to solve the non-linear problem by a succession of linear problems. With this aim, we first perform a time discretisation by an implicit Euler scheme and then we devise a fixed point iteration for the resulting non-linear problem.

5.1 The semi-discrete axial equation

Let us introduce a uniform time partition, $t_k = k\Delta t\,, k = 0, 1, \cdots, n$, where Δt is the time step and $t_n = t_e$, being $0 \leq t \leq t_e$ the time interval of interest. A semi-implicit Euler time advancing scheme applied to (16) and (22) reads

Given $T_E^{(0)} = T_E(0)$, for any $k = 0, 1, \cdots, n-1$, seek $T_E^{(k+1)} \approx T_E(t_{k+1}) : [0, L] \to \mathbb{R}$, such that

$$\begin{aligned} & \frac{1}{\Delta t} C(x; T_E^{(k+1)}) - \frac{d}{dx} K(x; T_E^{(k+1)}) + \alpha (T_E^{(k+1)})^4 \\ = \; & \frac{1}{\Delta t} C(x; T_E^{(k)}) + (Q(x; T_E) + \alpha T_a^4 + f_g)^{(k)}(x; T_E)\,, \end{aligned} \tag{24}$$

with

$$\begin{cases} K(0; T_E^{(k+1)}) = S_t\, e\sigma((T_E)^{(k)^4} - T_a^4) & \text{at } x = 0 \\ T_E^{(k+1)} = T_L(t_{k+1}) & \text{at } x = L. \end{cases} \tag{25}$$

Notice that Q and f_g are treated explicitly to ease the complexity of the non-linear problem. Indeed, the non-linear dependence of Q on the temperature T_E would be difficult to treat in an implicit fashion. On the other hand, the f_g term is usually of smaller importance with respect to the other terms (at least for the usual glow-plug geometries), thus its explicit treatment is not critical for the stability of the scheme. This is particularly true for the simulation of the transient, where the computation would require very small Δt anyway. As before we have indicated the dependence of the various terms on T_E and (thanks to the variable coefficients) on x.

We will treat all the implicit terms in a self-consistent fashion through fixed-point iterations.

5.2 Linearisation of the semi-discrete equation

The semi-discrete equation (24) can be cast in the general setting of a second order conservation law for the unknown $u := T_E^{(k+1)}$, as follows:

$$-\frac{d}{dx} K(x; u) + s(x; u) = f(x)\,, \quad x \in (0, L), \tag{26}$$

with

$$\begin{cases} K(0; u) - S_t \sigma e\, u^4 = S_t \sigma e\, T_a^4 & \text{at } x = 0 \\ u(L) = T_L(t_{k+1}) & \text{at } x = L. \end{cases} \tag{27}$$

Here,

$$s(x;u) = \frac{1}{\Delta t} C(x;u) + \alpha(x) u^4 \,, \tag{28}$$

$$f(x) = \frac{1}{\Delta t} C(x; T_E^{(k)}(x)) + Q(x; T_E^{(k)}(x)) + \alpha(x) T_a^4 + f_g\left(x; T_E^{(k)}(x)\right) \tag{29}$$

Notice that $T_E^{(k)}$ is here a known quantity. From (18) that we may write

$$K(x;u) = h_1(x;u) + h_2(x;u)\frac{du}{dx}, \tag{30}$$

where

$$h1(x;u) = \kappa_O(u)\frac{\partial \overline{T}_O^A}{\partial x}(x;u) + \kappa_G(u)\frac{\partial \overline{T}_G^A}{\partial x}(x;u), \tag{31}$$

$$h2(x;u) = \left(\kappa_O(u)\frac{\partial \overline{T}_O^A}{\partial u}(x;u) + \kappa_G(u)\frac{\partial \overline{T}_G^A}{\partial u}(x;u)\right). \tag{32}$$

We remind that the expressions for $\overline{T}_O^A$ and $\overline{T}_G^A$ are found in (13).

We shall solve (26) in an iterative fashion. Let us introduce the iteration index j. Starting from a given u_0, we want to build a sequence of approximations u_j, $j = 0, 1, \ldots$ with the property that $u = \lim_{j\to\infty} u_j$. At each step of the iterative algorithm we compute u_{j+1} by solving a linear system obtained from (26) by approximating the terms h and s using a first-order Taylor expansion around u_j. The same technique is adopted to linearise the radiation boundary term.

If we computed the exact Jacobian at each iteration j, we would obtain the well known Newton method. Its computational complexity led us to select instead a quasi-Newton technique where the Jacobian is approximated by discarding a few terms following some stability considerations. This method has also the advantage that the existence and uniqueness of the intermediate solutions is assured by classical results. Clearly we will ensure that, provided that convergence occurs, the limiting solution still coincides with u, i.e., we do not lose consistency.

Let us use the following notation $w_j = \frac{du_j}{dx}$, $U_j = u_{j+1} - u_j$ and $h(u_j, w_j) = h_1(u_j) + h_2(u_j)w_j$, where, for the sake of simplicity, we have dropped the dependence on x (which is however understood). A Newton iteration applied to (26) would read:

given u_0, for $j \geq 0$, compute $u_{j+1} = u_j + U_j$ where U_j satisfies

$$-\frac{d}{dx}\left[D_w h(u_j, w_j)\frac{d}{dx}U_j\right] - \frac{d}{dx}\left[D_u h(u_j, w_j)U_j\right] + D_u s(u_j)U_j = -F(u_j, w_j). \tag{33}$$

Here, D_y is the Fréchet derivatives with respect to y, while

$$F(u, w) = -\frac{d}{dx}h(u, w) + s(u) - f(u) \tag{34}$$

is the residual, which should be driven to zero by the procedure. Clearly, (33) is supplemented by the boundary terms, whose discussion is postponed. Let us first note that (33) is a linear transport-diffusion-reaction problem. In order to simplify calculations we take the following steps

1. We discard the "transport term" $\frac{d}{dx}\left[D_u h(u_j, w_j) U_j\right]$ to avoid the need of using stabilized finite elements to solve (33).

2. We neglect all contributions to $D_w h(u_j, w_j)$ and $D_u s(u_j)$ that would possibly make these operator indefinite. More precisely, we will ensure that the operator in the left-hand side of (33) is positive definite.

Let us analyze point 2. in more detail. From (32) we have

$$D_w h = h_2 = \kappa_O \frac{\partial \overline{T}_O^A}{\partial u} + \kappa_G \frac{\partial \overline{T}_G^A}{\partial u},$$

while (13) gives

$$\begin{aligned} \frac{\partial \overline{T}_O^A}{\partial u} &= \beta_O + 4\,\alpha\,\gamma_O\,u^3 + \alpha \frac{\partial \gamma_O}{\partial u}(u^4 - T_a^4)\,, \\ \frac{\partial \overline{T}_G^A}{\partial u} &= \beta_G + 4\,\alpha\,\gamma_G\,u^3 + \alpha \frac{\partial \gamma_G}{\partial u}(u^4 - T_a^4)\,. \end{aligned} \tag{35}$$

Since we are using absolute temperatures, any physical solution of our problem would satisfy $u = T_E^{(k+1)} > 0$, for all k. Thus, the only terms whose sign is not a-priori non-negative are the ones involving $\frac{\partial \gamma_O}{\partial u}$ and $\frac{\partial \gamma_G}{\partial u}$, which are therefore discarded. The analogous terms are discarded in

$$D_u s = \frac{1}{\Delta t}\left(C_O \frac{\partial \overline{T}_O^A(x;u)}{\partial u} + C_G \frac{\partial \overline{T}_G^A}{\partial u}(x;u) \right) + 4\alpha(x) u^3\,, \tag{36}$$

thus guaranteeing the positiveness of the operators.

In conclusion, the j-th iterate of the proposed quasi-Newton method is

$$-\frac{d}{dx}\left(\mathcal{K}_j(x)\,\frac{d}{dx} U_j \right) + \mathcal{S}_j(x)\,U_j = \mathcal{F}_j(x)\,, \tag{37}$$

where

$$\begin{aligned} \mathcal{K}_j(x) &= \kappa_O(u(x))\left[\beta_O(x) + 4\,\alpha(x)\,\gamma_O(x;u(x))\,u_j^3(x)\right] \\ &+ \kappa_G(u(x))\left[\beta_G(x) + 4\,\alpha(x)\,\gamma_G(x;u(x))\,u^3(x)\right], \\ \mathcal{S}_j(x) &= 4\,\alpha(x)\,u^3(x) + \frac{C_O}{\Delta t}\left[\beta_O(x) + 4\,\alpha(x)\,\gamma_O(x;u(x))\,u^3(x)\right] \\ &+ \frac{C_G}{\Delta t}\left[\beta_G(x) + 4\,\alpha(x)\,\gamma_G(x;u(x))\,u^3(x)\right], \\ \mathcal{F}_j(x) &= \frac{d}{dx}\left(h(x;u_j,w_j)\frac{du}{dx} \right) - s(x;u_j) + f(x;u_j). \end{aligned} \tag{38}$$

For the sake of completeness, the dependence on x has been made here explicit (we recall that u_j and $w_j = \frac{du_j}{dx}$ are known functions of x).

5.3 Boundary terms

Finally, we need to discuss the implementation of the boundary conditions. First, we assume that u_0 has been chosen so that it satisfies the Dirichlet boundary condition. Then the boundary condition for U_j at $x = L$ becomes the homogeneous condition $U_j(L) = 0$, for all $j \geq 0$. As for the radiation condition at $x = 0$, starting from the expression found in (27) and linearising around the state $u = u_j$, by making the same assumptions stated above, we have

$$\mathcal{K}\frac{d}{dx}U_j - 4S_te\,\sigma u_j^3 U_j = -\left[h\Big(x, u_j, \frac{d}{dx}u_j\Big) - S_te\,\sigma\Big(u_j^4 - T_a^4\Big)\right] \quad \text{at } x = 0\,. \tag{39}$$

That is, condition (27) has been approximated by a linear Robin boundary condition.

5.4 The quasi-Newton iteration

The problem to solve at every quasi-Newton iteration for the computation of the temperature profile at $t = t_{k+1}$ is then

$$\begin{cases} -\dfrac{d}{dx}\left[\mathcal{K}_j(x)\,\dfrac{d}{dx}U\right] + \mathcal{S}_j(x)\,U = \mathcal{F}_j(x) & x \in (0, L), \\ \mathcal{K}_j(x)\dfrac{dU}{dx} - 4S_te\,\sigma u_j(x)^3 U = -h(x, u_j, \dfrac{d}{dx}u_j) + S_te\,\sigma u_j^4 - T_a^4 & \text{at } x = 0, \\ U = 0 & \text{at } x = L, \end{cases} \tag{40}$$

which is a standard elliptic problem with mixed boundary conditions whose analysis is standard, see for instance [7].

In the following we drop, for the sake of simplicity, the iteration index j for U_j. The iterative procedure to compute T_E at time $t = t_{k+1}$ thus reads:

Choose a suitable u_0 that satisfies the Dirichlet boundary condition $u_0(L) = T_E(L, t_{k+1})$, and a tolerance $\tau > 0$,

1. for $j = 0, \ldots$
2. solve (40)
3. set $u_{j+1} = u_j + U$
4. If $\|U\| \leq \tau$ set $T_E^{(k+1)} = u_{j+1}$, and exit.

Here $\|U\|$ indicates a suitable norm, typically the $H1$ norm. If the iteration converges it converges to the solution of the non-linear problem.

6 A finite element scheme for the linearized problem

We address in the following the variational formulation of problem (40) and its associated finite element discretisation. For ease of notation, we drop henceforth

the suffix j and the dependence on x of the coefficients as well as of the right-hand side will be understood.

We have to solve the following boundary-value problem for the unknown u,

$$\begin{cases} -\dfrac{d}{dx}\left(\mathcal{K}\dfrac{du}{dx}\right) + \mathcal{S}u = \mathcal{F}\,, & x \in (0,L)\,, \\ \mathcal{K}\dfrac{du}{dx} - au = -b\,, & x = 0\,, \\ u = 0\,, & x = L\,, \end{cases} \tag{41}$$

where

$$\begin{aligned} a &= 4S_t e\,\sigma u_j^3\big|_{x=0} \quad \text{and} \\ b &= \left[h\Big(x, u_j, \frac{d}{dx}u_j\Big) - S_t e\,\sigma(u_j^4 - T_a^4)\right]\Big|_{x=0}. \end{aligned}$$

A standard finite element discretisation of (41) would provide a direct approximation $u_h \in C^0(0,L)$ of the primal variable u on a given partition $\mathcal{T}_h$ of the computational domain Ω. As a consequence, the approximate heat flux $q_h = -\mathcal{K}\frac{d\,u_h}{d\,x}$ is a *post-processed* quantity, and its accuracy would not be optimal because of the numerical differentiation process. Moreover, q_h turns out to be in general a *discontinuous* function, because of the jumps of $\frac{d\,u_h}{d\,x}$ across elements. Furthermore the discrete problem would not satisfy the conservation property at elemental level, but only globally.

Because of the nature of this problem, we are instead looking for a finite element formulation which is at the same time computationally efficient and allows to enforce energy conservation at local level.

To that goal, a mixed formulation of problem (41) is preferable, since here it is easier to ensure local energy conservation [2] as the heat flux

$$q = -\mathcal{K}\,\frac{du}{dx} \tag{42}$$

is an additional unknown of the problem, which is reformulated (41) as the following system of first-order equations in conservation form,

$$\begin{cases} \dfrac{1}{\mathcal{K}}\,q + \dfrac{du}{dx} = 0\,, & x \in (0,L)\,, \\ \dfrac{dq}{dx} + \mathcal{S}u = \mathcal{F}\,, & \text{in } \Omega\,, \\ q + au = b\,, & x = 0\,, \\ u = 0\,, & x = L\,. \end{cases} \tag{43}$$

Problem (43) is the so-called *mixed strong formulation* of the boundary value problem (41)[2], due to the simultaneous presence of the *primal unknown* u (the temperature) and of the associated *dual unknown* q (the heat flux). In contrast to this definition, (41) is called *primal formulation.*

6.1 The dual-mixed variational formulation

The weak (or variational) formulation of (43) is obtained by standard means [2], and reads as follows:

Find $q \in Q$ and $u \in V$ such that

$$\begin{cases} \displaystyle\int_0^L \frac{1}{\mathcal{K}}\, q\tau \, dx - \int_0^L u \frac{d\tau}{dx}\, dx + \frac{\tau(0)q(0)}{a} = \frac{\tau(0)b}{a}, & \forall \tau \in Q, \\ \displaystyle -\int_0^L v \frac{dq}{dx}\, dx - \int_0^L \mathcal{S} uv \, dx = -\int_0^L \mathcal{F} v \, dx\,, & \forall v \in V\,. \end{cases} \tag{44}$$

where Q and V are the appropriate functional spaces for the problem to hand, namely the Hilbert spaces

$$V = L^2(\Omega), \quad \text{and } Q = H^1(\Omega) = \left\{ f \in L^2(\Omega) \,|\, df/dx \in L^2(\Omega) \right\}.$$

Here $L^2(\Omega)$ denotes the space of square integrable functions over Ω and df/dx has to be taken in a distributional sense [7].

It can be verified by standard arguments [7] that (44) admits a unique solution $(u, q) \in (V \times Q)$ and that, under appropriate regularity assumptions, this pair is also the solution of (41) and $q = -\mathcal{K}\, du/dx$. System (44) is more usually called *dual-mixed* (DM) *weak formulation* of problem (41), since the two equations in (44) are the Euler-Lagrange equations emanating from the dual problem. If we define the *complementary energy*

$$E^*(\tau, v) = \int_0^L \frac{1}{2\mathcal{K}}\, \tau^2 - \left(\frac{d\tau}{dx} + \frac{\mathcal{S} v}{2} - \mathcal{F} \right) v \, dx + \frac{1}{a}\tau(0) \left(\frac{\tau(0)}{2} - b \right), \tag{45}$$

we have that

$$E^*(q, u) = \inf_{\tau \in Q} \sup_{v \in V} E^*(\tau, v).$$

6.2 Finite element approximation of the DM formulation

Let us introduce a nonuniform partition $\mathcal{T}_h$ of the computational domain $\Omega = (0, L)$ into intervals (elements) $K_i = (x_i,\, x_{i+1})$, with $i = 1, \ldots, N_h$, such that $x_1 = 0 < x_2 < \ldots < x_{N_h} < x_{N_h+1} = L$. We also define $x^i = (x_i + x_{i+1})/2$, $i = 1, \ldots, N_h$, and denote by h_i the width of K_i. Finally, $h = \max_{1 \le i \le N_h} h_i$. Given an integer $k \ge 0$ and an interval K, we denote by $P_k(K)$ the space of polynomials of degree less than or equal to k defined on K. Then we introduce the following finite dimensional spaces:

$$V_h = \{ v_h \in V \,|\, v_h \in P_0(K) \quad \forall K \in \mathcal{T}_h \},$$

$$Q_h = \{ \tau_h \in Q \,|\, v_h \in P_1(K) \quad \forall K \in \mathcal{T}_h \}.$$

Clearly, $V_h \subset V$ and $Q_h \subset Q$. The pair (V_h, Q_h) is known as the Raviart-Thomas finite element space RT_0, which is the one of lowest degree among the Raviart-Thomas finite element family and is probably the most widely used finite element

space for dual-mixed formulations. Notice that functions belonging to V_h are piecewise constant, while functions in Q_h are piecewise linear and continuous. The finite element approximation of problem (44) reads:

Find $q_h \in Q_h$ and $u_h \in V_h$ such that, for any $(\tau_h, v_h) \in Q_h \times V_h$

$$\begin{cases} \displaystyle\int_0^L \frac{1}{\mathcal{K}}\, q_h \tau_h \, dx - \int_0^L u_h \frac{d\tau_h}{dx}\, dx + \frac{\tau_h(0) q_h(0)}{a} = \frac{\tau_h(0) b}{a}, \\ \displaystyle -\int_0^L v_h \frac{dq_h}{dx}\, dx - \int_0^L \mathcal{S} u_h v_h \, dx = -\int_0^L \mathcal{F} v_h \, dx\,. \end{cases} \tag{46}$$

It is possible to verify that the above problem admits a unique solution, and it can be proved that q_h and u_h converge optimally to the corresponding quantities q and u [2]. Moreover, the computed heat flux q_h is continuous and satisfies the thermal equilibrium equation locally, i.e. over each finite element (provided that $\mathcal{S}$ and $\mathcal{F}$ are integrated exactly), unlike the case of a primal-based formulation. The matrix form of (46) is

$$\begin{pmatrix} A & B^T \\ B & C \end{pmatrix} \begin{pmatrix} \mathbf{q} \\ \mathbf{u} \end{pmatrix} = \begin{pmatrix} \mathbf{g}_1 \\ \mathbf{g}_2 \end{pmatrix}\,, \tag{47}$$

where $A \in \mathbb{R}^{(N_h+1)\times(N_h+1)}$, $B \in \mathbb{R}^{N_h \times (N_h+1)}$ and $C \in \mathbb{R}^{N_h \times N_h}$, while $\mathbf{q} \in \mathbb{R}^{N_h+1}$, $\mathbf{u} \in \mathbb{R}^{N_h}$, $\mathbf{g}_1 \in \mathbb{R}^{N_h+1}$ and $\mathbf{g}_2 \in \mathbb{R}^{N_h}$.

The algebraic structure in (47) requires a relatively intensive computational effort for the solution of the linear system. With respect to more standard finite elements employing the primal formulation, we have here the vector $\mathbf{q}$ additional unknowns. Yet, by some special techniques it is possible to reduce the computational cost to a level comparable to that of primal type formulations, as we will detail in the following section.

6.3 Efficient implementation of the DM formulation through elimination of the flux variable

Looking system (47) in more detail we may note that the matrix A is symmetric, tridiagonal and positive definite, while C is diagonal and negative. Clearly, the fact that A is *not* diagonal makes it impossible to eliminate $\mathbf{q}$ in a simple way. Yet this problem may be overcome by performing a suitable diagonalisation of A.

First, let us write out the entries of A explicitly,

$$A_{ij} = \begin{cases} \displaystyle\int_{K_1} \frac{1}{\mathcal{K}}\, \tau_j \tau_1 \, dx, & i = 1, \\ \displaystyle\int_{K_{i-1}} \frac{1}{\mathcal{K}}\, \tau_j \tau_i \, dx + \int_{K_i} \frac{1}{\mathcal{K}}\, \tau_j \tau_i \, dx, & i = 2, \ldots, N_h, \\ \displaystyle\int_{K_{N_h}} \frac{1}{\mathcal{K}}\, \tau_j \tau_{N_h+1} \, dx, & i = N_h + 1, \end{cases} \tag{48}$$

where $1 \le j \le N_h + 1$.

The exact computation of the integrals in (48) is in general unpractical (if not impossible) since $\mathcal{K}$ is a rather involved function of x. It is then convenient to approximate the thermal conductivity $\mathcal{K}$ on each element $K_i \in \mathcal{T}_h$, $i = 1, \ldots, N_h$, with a constant value $\mathcal{K}_i$, here defined as the midpoint value of $\mathcal{K}$. By doing so, the matrix A is replaced by the approximation $\widetilde{A}$ whose entries can be computed explicitly,

$$\widetilde{A}_{ij} = \begin{cases} \dfrac{1}{\mathcal{K}_1} \displaystyle\int_{K_1} \tau_j \tau_1 \, dx, & i = 1, \\ \dfrac{1}{\mathcal{K}_{i-1}} \displaystyle\int_{K_{i-1}} \tau_j \tau_i \, dx + \dfrac{1}{\mathcal{K}_i} \displaystyle\int_{K_i} \tau_j \tau_i \, dx, & i = 2, \ldots, N_h, \\ \dfrac{1}{\mathcal{K}_{N_h}} \displaystyle\int_{K_{N_h}} \tau_j \tau_{N_h+1} \, dx, & i = N_h + 1 \end{cases} \tag{49}$$

with $j = 1, \ldots, N_h + 1$.

Matrix $\widetilde{A}$ is symmetric and tridiagonal; in addition it immediately turns out that is also positive definite. To reduce it to a diagonal form we evaluate the integrals in (49) by using a trapezoidal quadrature rule (a technique widely known as *lumping*), obtaining the following entries for the diagonal matrix $\widehat{A}$,

$$\widehat{A}_{ii} = \begin{cases} \dfrac{h_1}{2\mathcal{K}_1}, & i = 1, \\ \dfrac{h_{i-1}}{2\mathcal{K}_{i-1}} + \dfrac{h_i}{2\mathcal{K}_i}, & i = 2, \ldots, N_h, \\ \dfrac{h_{N_h}}{2\mathcal{K}_{N_h}} & i = N_h + 1. \end{cases} \tag{50}$$

It can be shown that the above approximation does not alter the optimal convergence properties of the DM finite element scheme [5], while it allows to eliminate easily the heat flux degrees of freedom $\mathbf{q}$ from (47). First, we write

$$\mathbf{q} = \widehat{A}_h^{-1}(\mathbf{g}_1 - B^T \mathbf{u}), \tag{51}$$

then we substitute this expression into $(47)_2$, yielding the following linear system for $\mathbf{u}$,

$$(B\widehat{A}_h^{-1}B^T - C)\mathbf{u} = B\widehat{A}_h^{-1}\mathbf{g}_1 - \mathbf{g}_2. \tag{52}$$

The matrix $B\widehat{A}_h^{-1}B^T - C$ is tridiagonal, symmetric and positive definite. The heat fluxes are then recovered back using (51), once $\mathbf{u}$ has been computed from (52).

The reduced system (52) can be interpreted as a *finite volume scheme* for the temperature field u operating on the staggered grid defined by the midpoints of the partition $\mathcal{T}_h$. It is also interesting to notice that the use of the trapezoidal quadrature rule, combined with the piecewise constant approxima-

tion of $\mathcal{K}$, yields the following expression for the nodal fluxes

$$q_i = \begin{cases} -\dfrac{u_1 - \frac{b}{a}}{\frac{h_1}{2\mathcal{K}_1} + \frac{1}{a}}, & i = 1, \\ -H_i(\mathcal{K}_{i-1}, \mathcal{K}_i)(u_i - u_{i-1}), & i = 2, \ldots, N_h, \\ \dfrac{2u_{N_h}\mathcal{K}_{N_h}}{h_{N_h}} & i = N_h + 1, \end{cases} \tag{53}$$

where

$$H_i(\mathcal{K}_{i-1}, \mathcal{K}_i) = \frac{1}{\frac{h_{i-1}}{2\mathcal{K}_{i-1}} + \frac{h_i}{2\mathcal{K}_i}}, \qquad i = 2, \ldots, N_h\,,$$

is the *harmonic mean* of the heat conductivity $\mathcal{K}$. Harmonic averaging provides a superior accuracy and stability to the scheme, particularly when $\mathcal{K}$ changes rapidly [5, 1].

7 Numerical validation

Some preliminary numerical experiments have been carried out to validate the accuracy of the procedure proposed here. In the first example, we have solved the boundary-value problem (41) with the following choice of the coefficients and data: $L = 1$, $\mathcal{K}(x) = 1$, $\mathcal{S}(x) = 1$, $\mathcal{F}(x) = 2 + x - x^2$, $a = 1$, $b = 1$ and $u_L = 0$, having as exact solution the pair $u(x) = x(1 - x)$ and $q(x) = 2x - 1$. Since the exact heat flux is linearly varying, we expect good accuracy of the finite element formulation, where q_h is a piecewise linear continuous function over $\mathcal{T}_h$. This has been fully confirmed by the results shown in Fig. 5. In the second example, we

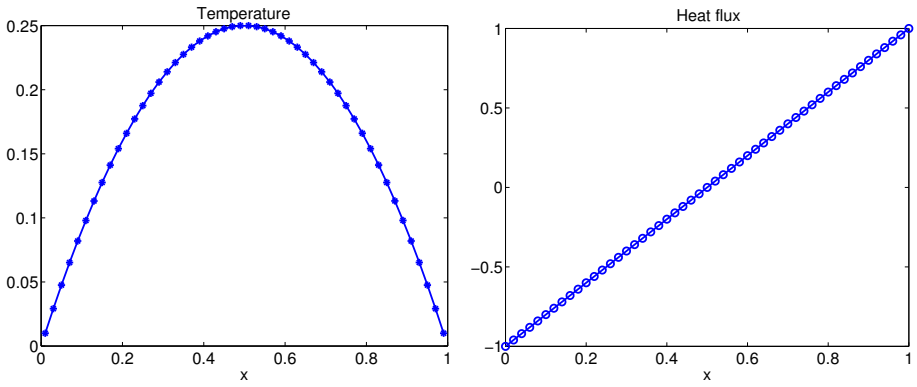

Figure 5: Finite element solution: u_h (left) and q_h (right)

have solved (41) with the following choice of the coefficients and data: $L = 5$, $\mathcal{K}(x) = 1$, $\mathcal{S}(x) = 1$, $\mathcal{F}(x) = e^{-x}(4x - 2)$, $a = 1$, $b = 0$ and $u_L = 25e^{-5}$, having as exact solution the pair $u(x) = x^2e^{-x}$ and $q(x) = -xe^{-x}(2 - x)$. We have

conducted an error analysis by taking a uniform mesh of grid size $h = 1/N_h$ with an increasing value of N_h in the range 2^k, $k = 1, \ldots, 8$. We show in Fig. 6 the curves of the discretisation errors $u - u_h$ and $q - q_h$ measured in the discrete maximum norm as

$$||u - u_h||_{\infty,h} = \max_{i=1,N_h} |u(x^i) - u^i|, \qquad ||q - q_h||_{\infty,h} = \max_{i=1,N_h+1} |q(x_i) - q_i|,$$

Second-order convergence with respect to the mesh parameter h can be neatly observed for *both* temperature and heat fluxes, which confirms the good convergence properties of mixed finite elements. The results of these preliminary

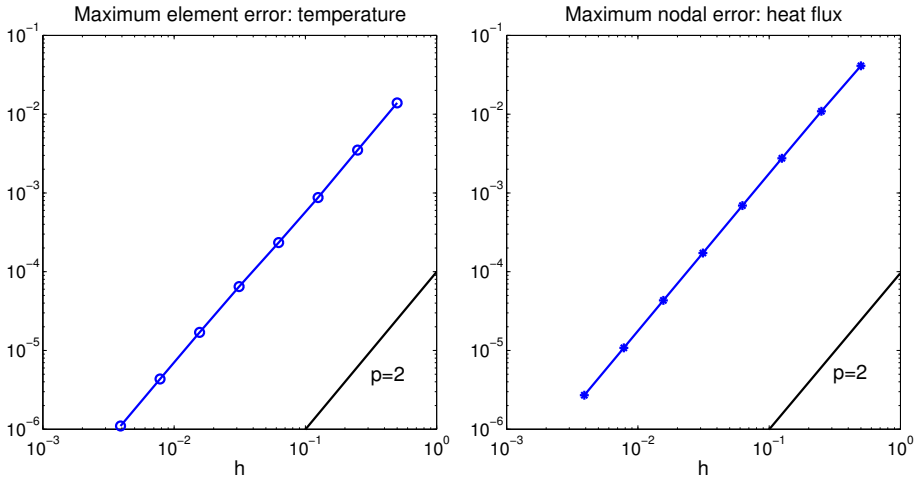

Figure 6: Logarithmic plots of $||u - u_h||_{\infty,h,E}$ and $||q - q_h||_{\infty,h,N}$

experiments have confirmed the validity of the numerical approach.

7.1 Comparison with experimental data

To validate the mathematical model we have carried numerical simulations on glow-plugs kindly provided by Federal Mogul Ignition S.r.l., of which experimental data was available. We are in the position of showing a typical result of this validation campaign. Figures 7-8 show two test cases for one type of glow-plug, here referred to as *GlowA*, associated with two different working conditions. The first test case corresponds to normal working conditions (Fig. 7) while the second one simulates the presence of a short-circuit at 14 [mm] from the tip and after 6 [s] from start-up (Fig. 8). The total length of the glow-plug is $L = 34\ mm$ and each figure displays, in left-right top-bottom order:

- the temperature T_E on the external steel covering as a function of the axial coordinate x. The different curve correspond to snapshots taken at successive time steps;
- the temperature T_E on the external steel covering at the coordinates x equal to 2, 4, 10, 14, 18, 22, 26, 30 and 34 millimeters, as a function of time;

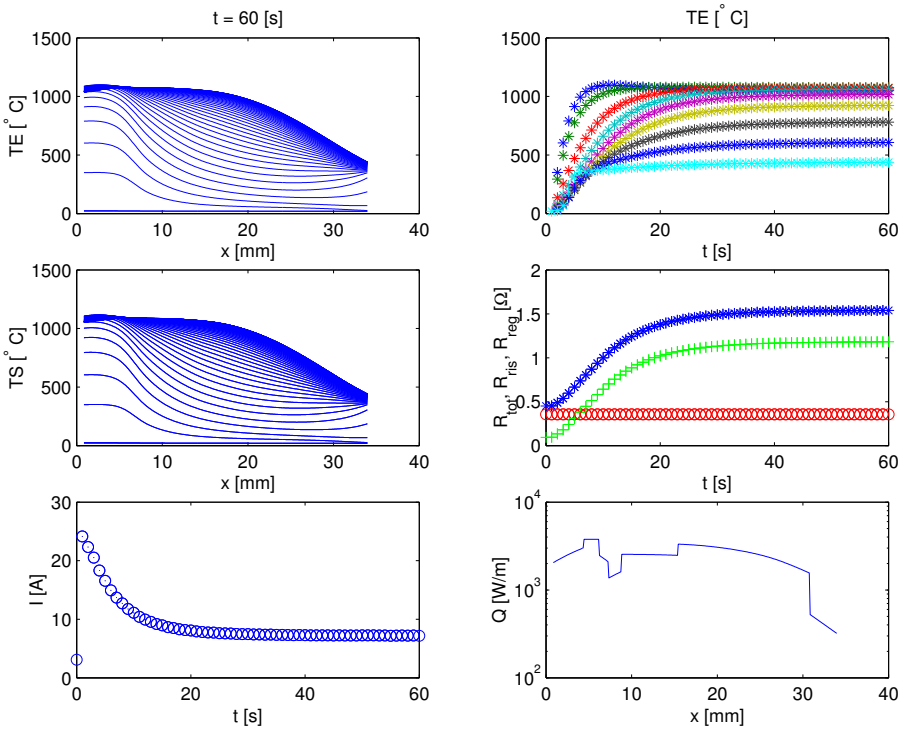

Figure 7: GlowA: simulation with no short-circuit

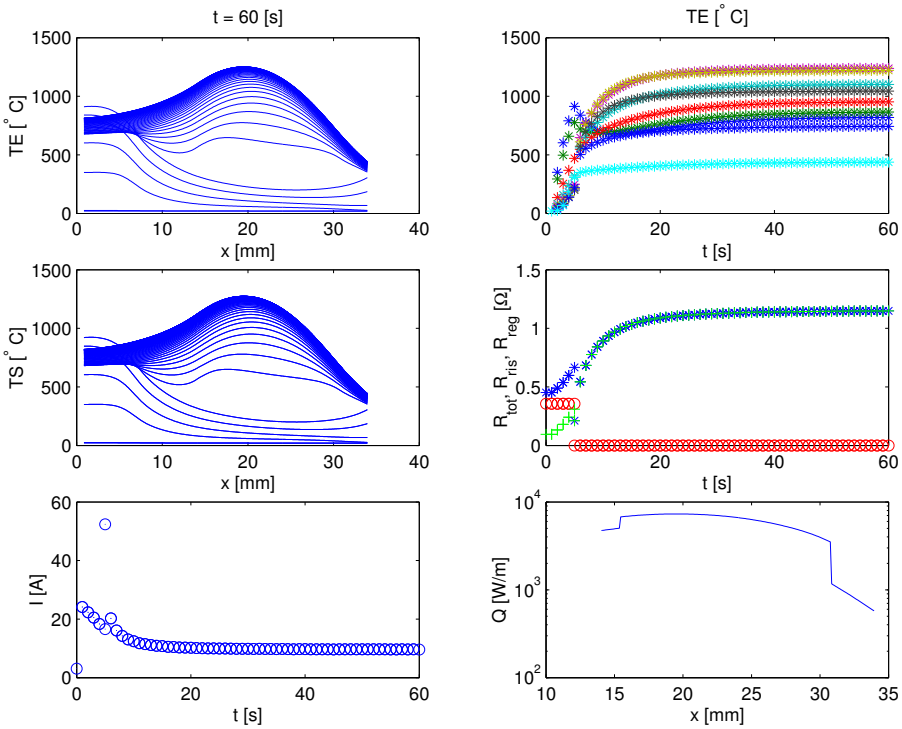

Figure 8: GlowA: simulation with a short-circuit at 14 [mm] after 6 [s]

- the temperature T_S on the coil as a function of x with snapshots at successive time steps;
- the values of the heating $\mathcal{R}_h$ (o), of the controlling $\mathcal{R}_l$ (+) and of the total $\mathcal{R}_C = \mathcal{R}_h + \mathcal{R}_l$ (*) resistances as functions of time;
- the current I in the coil as a function of time;
- the Joule power Q generated in the coil, per unit axial length.

On comparing the two cases, we notice in Fig. 8 the rapid raise of the electric current due to the decrease in the coil resistance as a consequence of the short-circuit. Notice also how in the short-circuited plug the temperatures T_E and T_S have a peak around $x = 20$ and decrease in the tip region because of the absence of the source of heat power. Finally, in Fig. 9 we compare in more detail

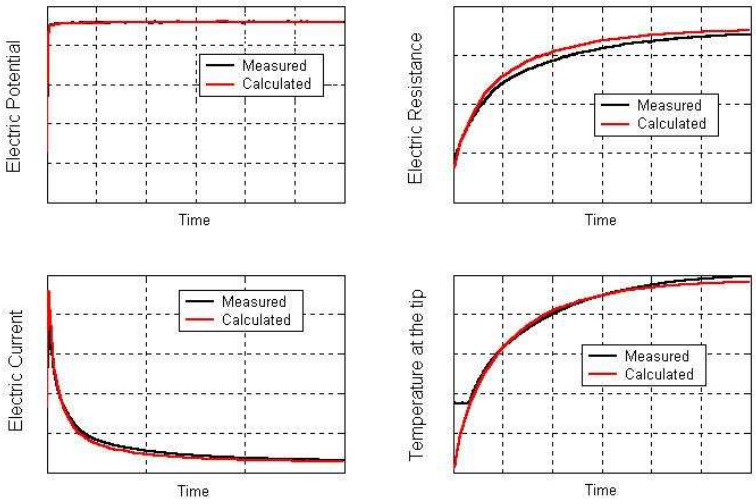

Figure 9: Some comparisons with experimental measurements

some of the computed quantities against their measured values, for the case of normal working conditions. More precisely, we show the total applied voltage ΔV (top-left), the total electric resistance $\mathcal{R}_C$ (top-right), the electric current I (bottom-left), and the temperature at the tip $T_E(0)$ (bottom-right), versus time. The very good matching between numerical results and experimental data can be appreciated.

As a final validation case we report in Fig. 10 the temperature at a point near the tip obtained in two realistic operating conditions, compared with the experimental measurements. In this simulation the heat transfer has been augmented by a term accounting for heat convection into the cylinder head. Indeed the velocity of the air-diesel fuel mixture flow around the plug is sufficiently high to make convective terms relevant. Convection introduces only a slight modification of the source term in the differential equation. Because of confidentiality

reasons, we cannot give more details nor show the actual temperature reached by the plug. Yet, the picture illustrates clearly the quality of the numerical result, which is able to reproduce, even in this more complex situation, the transient and the maximal temperature level.

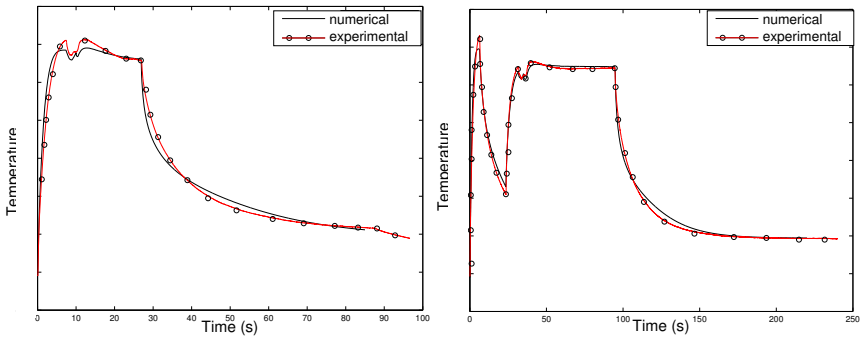

Figure 10: Comparisons with experimental measurements for two realistic operating conditions

8 Conclusions

This work demonstrate how it is possible to develop an effective and accurate tool to simulate a rather complex non-linear problem like the heating up process of a glow-plug. The software developed within this research activity is now operative in an industrial environment. Similar techniques may be adopted for other heating system with cylindrical geometries and where one dimension is dominant.

The use of mixed finite elements has proved important to obtain accurate results with a very good efficiency. Despite the fact that small time steps (of the order of 10^{-3} seconds) are needed to follow the transient, the code, written in MATLAB®, runs in a few seconds on a normal personal computer.

The authors wish to thank Federal Mogul Ignition S.r.l., and in particular Ing. R. Rossi, for the support and the availability of the experimental data.

Appendix

Aim of this appendix is the determination of dl/dx for common coil geometries. More precisely we will consider helical coils with cylindrical and conic geometries. We assume that the helix axis is perfectly aligned with x and the the helical pitch P_S is constant.

A Cylindrical helix

The parametric representation of the helix with constant pitch P_S with respect to the coordinate system of Fig. 11 (left), is

$$\begin{cases} y = y(\theta) = R_S \cos\theta\,, \\ z = z(\theta) = R_S \sin\theta\,, \\ x = x(\theta) = \dfrac{P_S}{2\pi}\,\theta\,, \end{cases} \quad , \quad 0 \le \theta \le 2\pi N,$$

where R_S is the radius of the helix, θ is the angle which parametrizes the helix, and N the number of spires (assumed to be an integer, for the sake of simplicity and without loss of generality). We then have

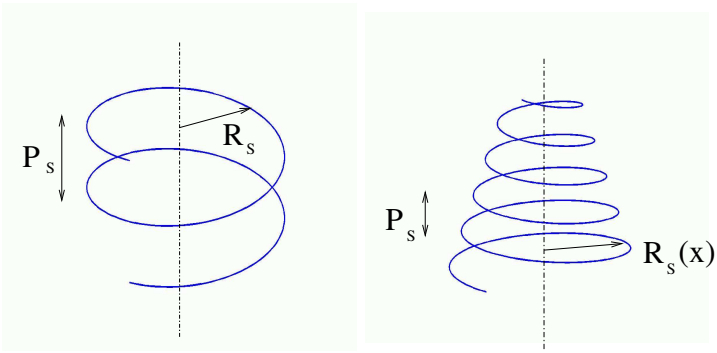

Figure 11: Geometry for the cylindrical (left) and of a conical (right) helix

$$\frac{dl}{d\theta} = \sqrt{R_S^2 + \frac{P_S^2}{4\pi^2}}.$$

Therefore,

$$\frac{dl}{dx} = \frac{dl}{d\theta}\frac{d\theta}{dx} = 2\pi\sqrt{\frac{R_S^2}{P_S^2} + \frac{1}{4\pi^2}}. \tag{54}$$

B Conic helix

The parametric representation is now given by, referring to Fig. 11 (right),

$$\begin{cases} y = y(\theta) = R_S(\theta)\cos\theta\,, \\ z = z(\theta) = R_S(\theta)\sin\theta\,, \\ x = x(\theta) = \dfrac{P_S}{2\pi}\,\theta\,, \end{cases}$$

where $R_S(\theta) = a\theta + b$ is the radius of the helix, here given as an affine function of θ depending on the constants a, b. P_S is again the helix pitch. In this case it is more convenient to re-parametrize the curve as a function of the axial coordinate x, as it follows

$$\begin{cases} y = y(x) = R_S(x)\cos\left(\frac{2\pi}{P_S}x\right)\,, \\ z = z(x) = R_S(x)\sin\left(\frac{2\pi}{P_S}x\right)\,, \end{cases}$$

where now $R_S(x) = Ax + b$, with $A = \frac{2\pi a}{P_S}$. Since,

$$\frac{dl}{dx} = \sqrt{1 + \left(\frac{dy}{dx}\right)^2 + \left(\frac{dz}{dx}\right)^2},$$

by carrying out the computations we obtain

$$\frac{dl}{dx}(x) = 2\pi\sqrt{\frac{R_S^2(x)}{P_S^2} + \frac{1}{4\pi^2}\left(1 + \left(\frac{dR_S}{dx}\right)^2\right)} = 2\pi\sqrt{\frac{R_S^2(x)}{P_S^2} + \frac{1}{4\pi^2}\left(1 + A^2\right)}\,.$$

Let us note that this expression generalizes (54) where $A = 0$. The expression for A and B may be derived in terms of the global dimensions of the helix. We denote by x_i and x_e the initial and final x coordinate of the entire conic helix under consideration, by $R_i = R_S(x_i)$ and $R_e = R_S(x_e)$ the corresponding values of the radius, and by $P_S = x_e - x_i$ the helix length. We have

$$R_S(x) = \frac{R_e - R_i}{P_S}(x - x_i) + R_i\,,$$

from which it follows that

$$A = \frac{dR_S}{dx} = \frac{R_e - R_i}{P_S}, \qquad B = \frac{R_i x_e - R_e x_i}{P_S}\,. \tag{55}$$

References

[1] I. Babuska and J. E. Osborn. Generalized finite element methods: their performance and their relation to mixed methods. *SIAM J. Numer. Anal.*, 20:510–536, 1983.

[2] F. Brezzi and M. Fortin. *Mixed and Hybrid Finite Element Methods.* Springer-Verlag, New York, 1991.

[3] A. Ern and J-L. Guermond. Accurate numerical simulation of radiative heat transfer with application to crystal growth. *Int. J. Numer. Meth. Engng.*, 61:559–583, 2004.

[4] J. Kusaka, Y. Daisho, and T. Saito. Ignition and combustion in a glow assisted d.i. methanol engine. In *X. Intl. Symposium on Alcohol Fuels Technology*, pages 871–878, 1992.

[5] S. Micheletti, R. Sacco, and F. Saleri. On some mixed finite element methods with numerical integration. *SIAM J. Sci. Comput.*, 23(1):245–270, 2001.

[6] J. Monnier and J.P. Vila. Convective and radiative thermal transfer with multiple reflections. analysis and approximation by a finite element method. *Math. Models Methods Appl. Sci.*, 11(2):229–261, 2001.

[7] A. Quarteroni and A. Valli. *Numerical Approximation of Partial Differential Equations.* Springer-Verlag, Berlin, 1984.

[8] M.L. Willi and B.G. Richards. Design and development of a direct injected, glow plug ignition assisted, natural gas engine. In *ASME Proceedings*, volume 22, pages 31–36, New York, 1994.

[9] H. Yui, N. Nakashima, and T. Shimada. Performance and exhaust gas characteristics of a glow plug assisted methanol diesel engine. In *VIII Intl. Symposium on Alcohol Fuels Technology*, pages 531–537, 1988.